Nine years of mass transport data in the eastern boundary of the North Atlantic Subtropical Gyre

Eugenio Fraile-Nuez,[1] Francisco Machín,[2] Pedro Vélez-Belchí,[1] Federico López-Laatzen,[1] Rafael Borges,[3] Verónica Benítez-Barrios,[3] and Alonso Hernández-Guerra[3]

Received 31 January 2010; revised 17 April 2010; accepted 18 May 2010; published 10 September 2010.

[1] One of the longest current meter time series in the Lanzarote Passage in the eastern boundary of the North Atlantic Subtropical Gyre has been used to determine and quantify the 9-year mean transport, the inter-annual and seasonal mass transport variability for the three water masses present in the area. Results show North Atlantic Central Water (NACW) flowing southward in the upper levels with a mean mass transport of −0.81 ± 1.48 Sv, Antarctic Intermediate Water (AAIW) flowing northward at intermediate levels with a mean transport of +0.09 ± 0.57 Sv and Mediterranean Water (MW) flowing southward in the deep part of the passage with a mean transport of −0.05 ± 0.17 Sv. Harmonic and wavelet analysis show the presence of a seasonal pattern in the passage for the three water masses. A maximum southward transport in winter and spring has been observed for the NACW followed by a minimum in summer and fall. Near zero values during winter and spring are found for AAIW, with a maximum northward value in summer and a negative value in fall, when this water mass reverses its flow. MW has a similar seasonal pattern to NACW. The vertical structure in the Lanzarote Passage can be approximated by four significant oscillatory modes which cumulatively explain 86.4% of the variance. The strong transport fluctuation found at the seasonal and inter-annual timescales demonstrates that the Eastern Boundary Current transport has a strong impact on meridional overturning estimates, thus indicating that to understand Meridional Overturning Circulation variability, these transport estimates at the eastern Atlantic margin are necessary.

Citation: Fraile-Nuez, E., F. Machín, P. Vélez-Belchí, F. López-Laatzen, R. Borges, V. Benítez-Barrios, and A. Hernández-Guerra (2010), Nine years of mass transport data in the eastern boundary of the North Atlantic Subtropical Gyre, *J. Geophys. Res.*, *115*, C09009, doi:10.1029/2010JC006161.

1. Introduction

[2] The Azores Current is the northernmost current in the Eastern North Atlantic Subtropical Gyre which turns south, splitting into several branches. The easternmost branch flows east of Madeira and supplies the Canary Current [*Siedler and Onken*, 1996; *Paillet and Mercier*, 1997; *Laiz et al.*, 2001; *Machín et al.*, 2006]. The Canary Current, flowing southwestward forced by the curl of the wind stress [*Fraile-Nuez and Hernández-Guerra*, 2006] and the meridional blocking of the African continent, constitutes the major Eastern Boundary Current (EBC) of the North Atlantic Subtropical Gyre.

[3] Particular effort was made during the CANIGO project (Canary Islands Azores Gibraltar Observations) [*Parrilla et al.*, 2002] to improve our understanding of the physics, biogeochemistry, and paleoceanography of the portion of the EBC that flows through the channel between the island of Lanzarote and the African coast (hereafter Lanzarote Passage, Figure 1) [*Hernández-Guerra et al.*, 2001, 2002, 2003; *Knoll et al.*, 2002; *Machín et al.*, 2006].

[4] The Lanzarote Passage is about 1300 m deep, and contains three water masses. The predominant upper-thermocline North Atlantic Central Water (NACW) is characterized by a close clustering of points in the θ/S diagram [*Wright and Worthington*, 1970; *Tomczak*, 1981]. It spans from the surface to the approximate neutral density value of 27.3 kg m^{-3} (roughly 600 m depth; neutral density, γ_n, as defined by *Jackett and McDougall* [1997] is used as the density variable throughout this work) [*Hernández-Guerra et al.*, 2001]. At intermediate levels, two water masses interleave in the EBC: Antarctic Intermediate Water (AAIW) and Mediterranean Water (MW). AAIW is found below the NACW, mainly between the layers 27.3 and 27.7 kg m^{-3}

[1]Centro Oceanográfico de Canarias, Instituto Español de Oceanografía, Santa Cruz de Tenerife, Spain.
[2]Institut de Ciènces del Mar, Barcelona, Spain.
[3]Facultad de Ciencias del Mar, Universidad de Las Palmas de Gran Canaria, Las Palmas de Gran Canaria, Spain.

0148-0227/10/2010JC006161

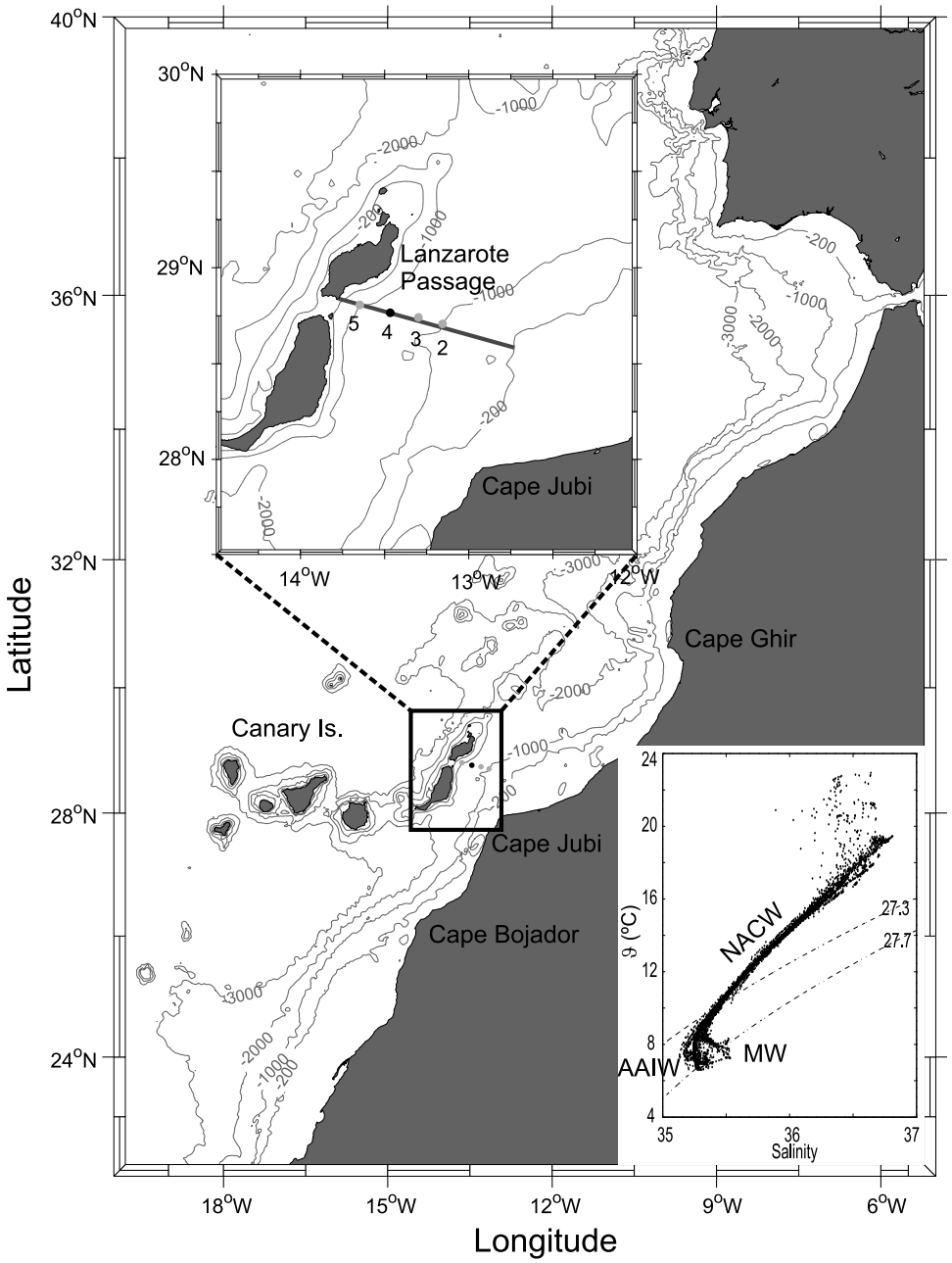

Figure 1. Eastern boundary of the North Atlantic Subtropical Gyre. Eastern Boundary Current (EBC) mooring positions are represented in the map and in the upper inset (zoom), where the Lanzarote Passage is shown. A black line across the moorings indicates the 12 occupations of the same hydrographic section carried out during these 9 years. For reference, the 200-, 1000-, 2000-, and 3000-m isobaths are shown [*Smith and Sandwell*, 1997]. In the lower inset, a θ/S diagram shows the distributions of the three water masses present in the area and used for this study.

(roughly 600–1100 m depth) with its core centered at 27.6 kg m^{-3} (roughly 900 m depth). AAIW is characterized by a minimum in salinity (S < 35.3). The MW reaches deeper than AAIW, roughly from 900 m to the bottom of the passage (γ_n > 27.45 kg m^{-3}) [*van Aken*, 2000; *Hernández-Guerra et al.*, 2003; *Machín and Pelegrí*, 2009]. The MW is characterized by maximum salinity (S > 35.5) values [*Arhan et al.*, 1994; *Hernández-Guerra et al.*, 2005; *Machín et al.*, 2006]. In the 1990s, several large-scale horizontal distributions of salinity, oxygen, and silica suggested a narrow northward penetration of AAIW along the eastern margin of the North Atlantic Subtropical Gyre, as the constant property lines stretch northeast along the African coastline. However, these were produced with rather low spatial resolution data that did not permit the identification of the spreading path [*Kawase and Sarmiento*, 1985; *Reid*, 1994; *Lozier et al.*, 1995]. Recently, this relatively fresh water flowing northward has been detected along the African slope as far north as 34°N during fall [*Machín and Pelegrí*, 2009].

Table 1. Summary of Mooring Information and Mean Flow Statistics for the 9-Year Time Series[a]

Depth (m)	Duration (days)	SPD (cm s^{-1})	DIR (°N)	u (cm s^{-1})	v (cm s^{-1})	vel_{mv} (cm s^{-1})	$rms_{(vel_m)}$	T (°C)	S	FKE (cm^2 s^{-2})	STAB
150	1797.0	6.1 ± 8.7 (3.9)	233.0 (216)	−4.9 ± 6.1 (−3.8 ± 5.6)	−3.7 ± 6.2 (−0.6 ± 4.9)	−6.0 ± 6.4	8.8	17.2 ± 0.7	36.3 ± 0.1	37.9 (27.6)	0.71 (0.57)
300	3135.0	4.2 ± 7.4 (4.1)	232.6 (254)	−3.3 ± 5.3 (−4.0 ± 6.1)	−2.5 ± 5.2 (−1.1 ± 4.2)	−4.1 ± 6.0	7.3	14.3 ± 0.5	36.2 ± 0.2	27.5 (27.9)	0.64 (0.61)
520	3001.1	2.0 ± 6.4 (2.1)	250.1 (268)	−1.8 ± 4.7 (−2.1 ± 4.4)	−0.7 ± 4.3 (−0.1 ± 3.2)	−1.8 ± 5.2	5.5	11.6 ± 0.2	35.7 ± 0.1	20.6 (14.8)	0.39 (0.47)
870	3152.7	0.9 ± 5.3 (1.1)	7.9 (33)	0.1 ± 3.9 (0.6 ± 4.5)	0.9 ± 3.5 (0.9 ± 2.7)	0.7 ± 4.5	4.6	8.3 ± 0.3	35.3 ± 0.1	13.9 (13.5)	0.21 (0.27)
1230	2274.3	1.2 ± 4.3 (1.3)	210.8 (238)	−0.6 ± 2.8 (−1.1 ± 3.7)	−1.0 ± 3.2 (−0.7 ± 2.4)	−1.2 ± 3.9	4.1	7.3 ± 0.3	35.4 ± 0.1	9.1 (9.9)	0.35 (0.35)

[a]*Hernández-Guerra et al.*'s [2003] values for the very first 4 years of the series are shown in parenthesis. SPD and DIR stand for the current mean speed and direction. Vel_{mv} indicates the velocity component projected to the principal angle along which the sum of the squares of the normal distance to the data points is minimum. FKE indicates the fluctuating part of vector variance or the kinetic energy per unit mass. STAB indicates the directional stability of the flow defined by the ratio of the magnitude of the mean vector to the mean speed.

[5] An element of the CANIGO project in the Lanzarote Passage was the deployment of four moorings with a total of 19 current meters from January 1997 to January 1999. Results from these observations, together with hydrographic and XBT cruises, gave a fairly comprehensive new picture of the circulation at the eastern boundary. The water masses found in the passage had a mean annual mass transports of −0.8 ± 1.1 Sv for NACW, +0.1 ± 0.4 Sv for AAIW and −0.05 ± 0.09 Sv for MW [*Hernández-Guerra et al.*, 2001, 2002, 2003; *Knoll et al.*, 2002]. After the CANIGO experiment, measurements in the Lanzarote Passage were continued with just one mooring representative of the whole passage [*Hernández-Guerra et al.*, 2003].

[6] The main purpose of the present study is on the one hand, to determine the seasonal and inter-annual dynamic variability of the EBC of the North Atlantic Subtropical Gyre and on the other hand, to demonstrate that the eastern Atlantic margin are necessary to understand the Meridional Overturning Circulation (MOC) variability. After a brief presentation of the collected hydrographic data in section 2 and current meter statistics in section 3, we will describe the vertical variability of the EBC in terms of a Empirical Orthogonal Function analysis in section 4, while the harmonic signals obtained in the time series are presented in section 5. The 9-year mean, the seasonal and inter-annual variability of the mass transport, are described in section 6 and our final results and discussion are given in section 7.

2. Data

2.1. Current Meter Description

[7] From January 1997 to January 1999, 19 current meters were installed on four moorings (Figure 1). The shallowest three current meters of each mooring were deployed at the thermocline water level occupied by NACW, the next (the next two for the case of EBC-2) at AAIW level, and the last for EBC-3 and EBC-4 at the MW level [*Hernández-Guerra et al.*, 2003]. Mooring EBC-4 is still maintained but we only show data until February 2006 due to a large gap of data from March 2006 to February 2008. Thus, a 9-year time series of velocity, temperature, salinity and pressure has been obtained from mooring EBC-4 from January 1997 to February 2006. The full 9-year record is analyzed in this study. Mooring EBC-4 is located at 28°44′N, 13°28′W in water of 1280 m depth (Figure 1). EBC-4 was initially equipped with 5 Aanderaa current meters, at approximately 150, 300, 520, 870 and 1230 m depth. During these 9 years the mooring has been recovered and deployed 11 times for maintenance.

[8] The sampling time interval for all current meters was 2 hours. All current meters returned good data for the 9 years with only minor gaps, except for the shallowest one where the gaps are substantial. Hence, the shallowest current meter is not used for the harmonic analysis and mass transport variability shown in sections 5 and 6. The time series were low-pass filtered with a cutoff period of 40 h to eliminate tidal and inertial signatures from the time series. Velocities were rotated to the principal angle, along which the sum of the squares of the normal distance to the data points is minimum [*Emery and Thomson*, 1998] as previously used in the Lanzarote Passage [*Hernández-Guerra et al.*, 2003].

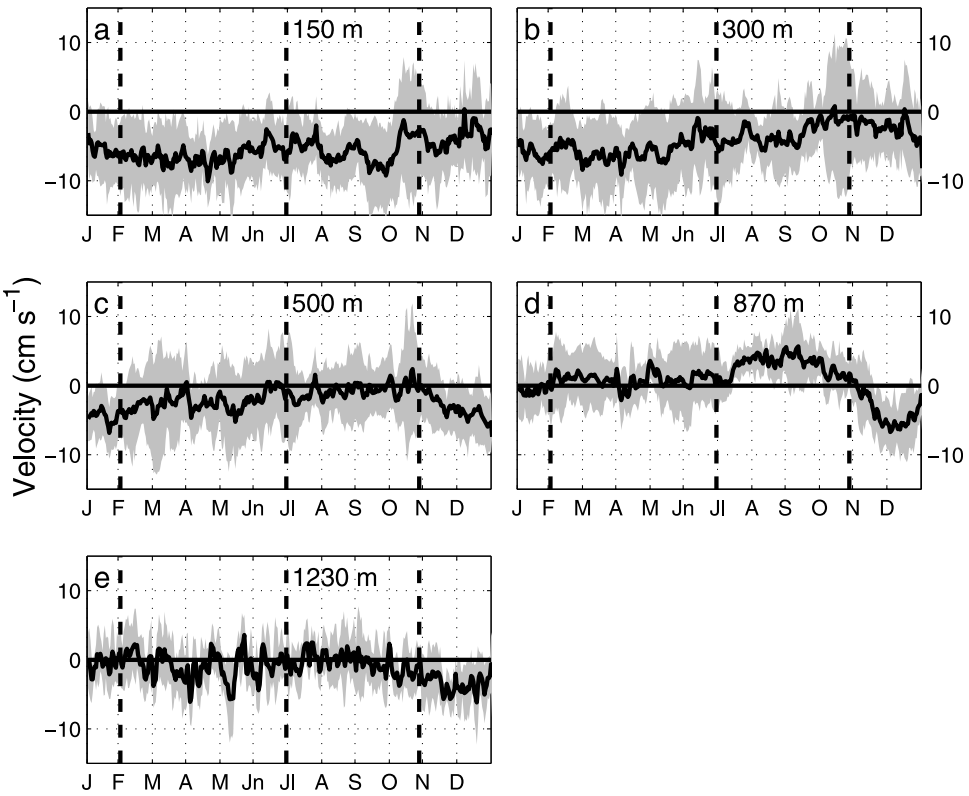

Figure 2. The 9-year average velocity distributions along the maximum variance axis at (a) 150, (b) 300, (c) 500, (d) 870, and (e) 1230 m. The standard deviation is shaded in gray.

2.2. Hydrographic Data

[9] From January 1997 to February 2006, the Lanzarote Passage has been occupied on 12 occasions (January and October 1997, March and July 1998, January and May 1999, April 2000, February 2001, February and September 2003, February both in 2005 and 2006). SeaBird 911+ CTD stations taken along this section were carried out from surface to bottom (Figure 1).

[10] Geostrophic transport is calculated for each occupation using two different levels of no motion, one located at the neutral density of 27.3 kg m^{-3} and a second one at the bottom. γ_n = 27.3 kg m^{-3} marks the limit between the NACW flowing southward and the AAIW flowing northward in the study area, so a level of no motion may be expected at this density level [*Hernández-Guerra et al.*, 2003]. Section 6 will compare these geostrophic transports to the transport time series from EBC-4.

3. Current Meter Statistics

[11] Table 1 shows the deployment information for each current meter for the mooring EBC-4. Also shown are the mean duration, velocity, direction, zonal and meridional components of the velocity, velocity projected to the principal angle and its root mean square, temperature, salinity, kinetic energy and the directional stability of the flow. Table 1 shows values quite similar to those reported by *Hernández-Guerra et al.* [2003] for the first four years of the series, but several minor differences are observed. The current meter located at the shallowest part of the water column now shows an increase of the kinetic energy and the stability for the current at this layer. The current meter at 500 m depth shows a decrease in the kinetic energy compared to the first four years of the series.

[12] The 9-year mean southward velocities in the range 5–10 cm s^{-1} are found at the first (~150 m) and second (~300 m) current meters, more intense during spring and weaker in summer and fall (Figure 2). The current meter located at 500 m depth has a mean velocity below 5 cm s^{-1} with a similar seasonality as the shallower current meters. On the other hand, the velocity pattern for the current meter located at the depth of the AAIW (~870 m) changes drastically. Near zero velocities with a small northward trend are found during February to June but from July to November a notable northward intensification of the velocity is found, with values up to 4–5 cm s^{-1}. From November to late December a drastic southward change of the direction of the velocity is found with sharp values around 5–6 cm s^{-1}. Finally, the signal found at the deeper current meter, 1230 m, is very variable and practically null although a southward net trend is found during November and December.

4. EOF Analysis

[13] A previous study in the area suggests a clear vertical structure as defined by NACW, AAIW and MW [*Müller and Siedler*, 1992]. In this section, we apply an Empirical Orthogonal Function (EOF) analysis to determine, first, to what extent the current in the passage can be described as either a two or three-layer domain and, secondly, the influence of the upwelling off northwest Africa on the dynamics of the Lanzarote Passage [*Hernández-Guerra and Nykjaer*, 1997].

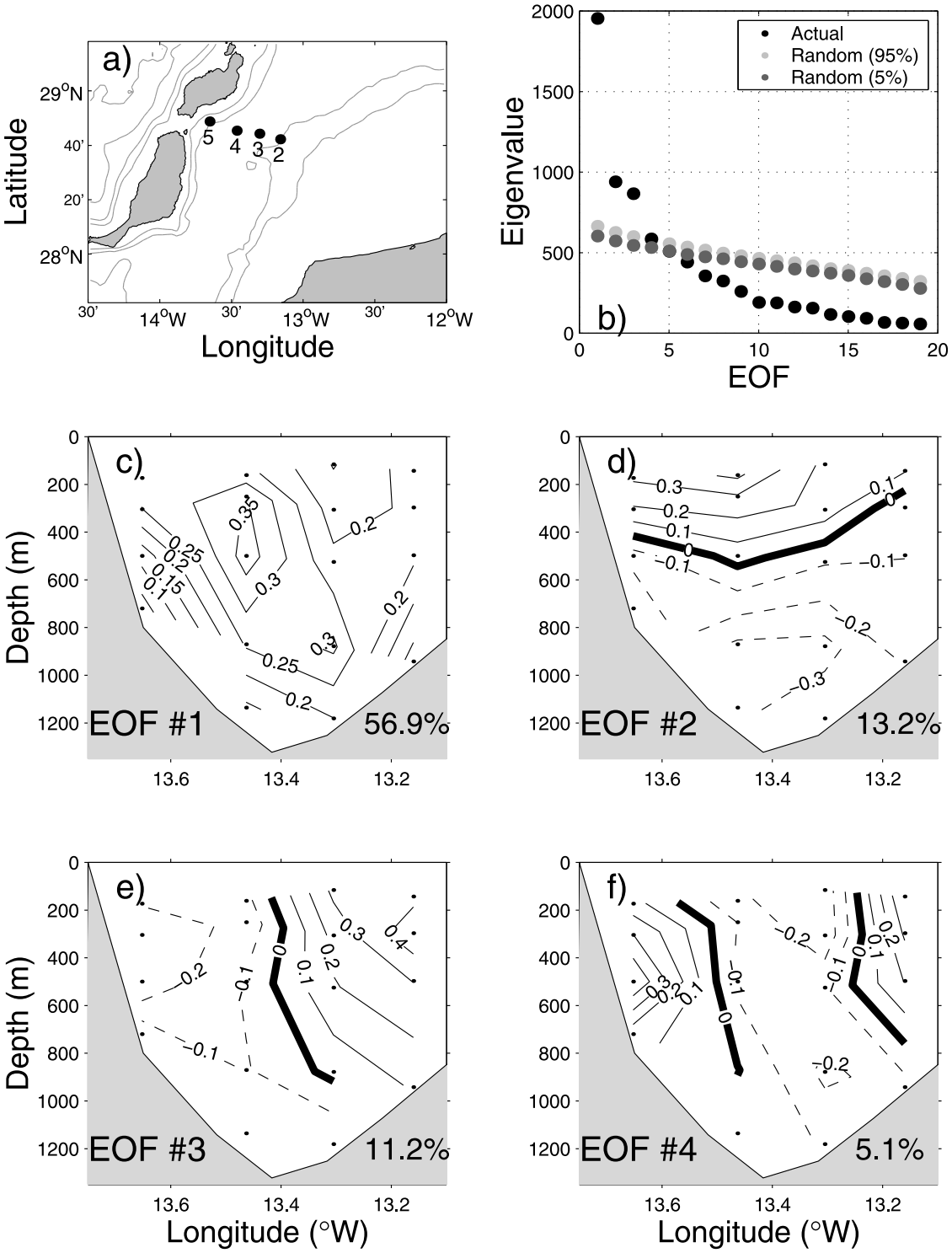

Figure 3. (a) A spatial Empirical Orthogonal Function (EOF) analysis is carried out with the two years of data from the 4 moorings installed in the Lanzarote Passage. (b) The Monte Carlo Method in order to determine the significant oscillation modes, (c–f) together with the total explained variance for each mode.

4.1. Temporal EOFs With Four Moorings

[14] A temporal EOF analysis has been done with the nineteen time series available for the passage from 1997 to 1999 (Figure 3a). The main aim of this EOF analysis is to find common oscillation patterns at all current meters, in order to describe the processes that force the observed variability of the time series and then try to quantify them.

[15] A Monte Carlo method has been applied as a significance test in order to determine the significant modes in

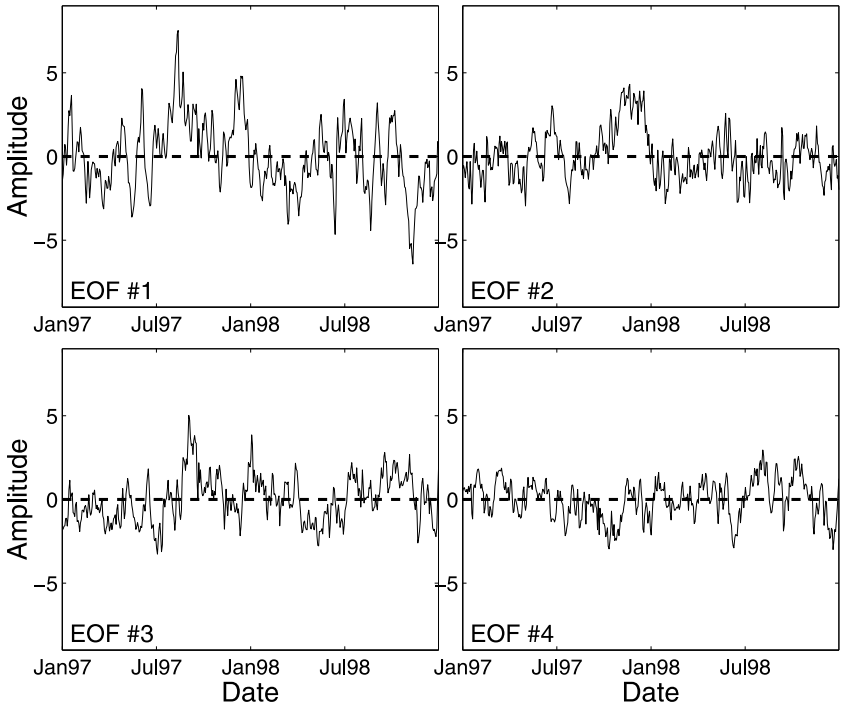

Figure 4. Temporal amplitude corresponding to the EOF analysis over the four EBC moorings.

the EOF analysis [*Hammersley and Handscomb*, 1964]. EOF analysis is performed 100 times with nineteen random time series with the same dimension of the original velocity time series. For every analysis, we store the different eigenvalues obtained from the noisy signal, so eigenvalues are considered as significant when they are above 95% of the eigenvalues generated from the noisy signal. Figure 3b presents the eigenvalues obtained from the original time series and from the random ones, where we can observe that four eigenvalues fall above the bounds given by the Monte Carlo analysis. These four significant oscillation modes cumulatively explain 86.4% of the overall variance.

[16] Figure 3c shows the first significant EOF that explains 56.9% of the variance of the data. This EOF contains positive values in the whole channel, with higher eigenvalues between 400–600 m depth and in the center of the passage, where EBC-4 is located. This pattern seems to be the combination of the barotropic mode with the first baroclinic mode of the quasi-geostrophic dynamics [*Müller and Siedler*, 1992]. The second significant mode that explains 13.2% of the variance, shows a double-cell circulation structure where the upper layer flows in the opposite direction to the intermediate one (Figure 3d). The depth of the interface between them roughly matches up with the lower part of the NACW in the passage [*Hernández-Guerra et al.*, 2003]. The depth of the interface is shallower at the eastern part of the passage where the upwelling off northwest Africa is located. The third significant mode explaining 11.2% of the data variance, marks a difference between the waters close to the continental slope and those close to the Canary Islands (Figure 3e). It seems to be related to the different dynamics between the northwest African upwelling system and the Canary Current. It is worth mentioning that the maximum values are found in the upper layer of the upwelling. The fourth significant mode, that explains just 5.1% of the data variance, presents a complex pattern with three vertical regions, one close to the islands, another at the center of the passage and finally one close to the continental shelf (Figure 3f).

[17] The amplitudes related to these EOFs are given in Figure 4. On the one hand, Figure 4 shows the higher amplitude in the first two modes with respect to the last two, indicating the greater importance of EOFs 1 and 2. On the other hand, a large temporal variability is observed in all of them, as was also observed in the original data set.

4.2. Temporal EOFs for the Nine-Year Record

[18] A temporal EOF analysis has been done with the 9-year EBC-4 time series applying the same method as that for the previous section. Figure 5a shows the significance test applied to the 9-year time series of the velocities. On this occasion, only two oscillation modes are significant. Figure 5b shows the vertical distribution of significant eigenvectors. These two first significant oscillation modes have a similar interpretation as described in section 4.1 for the EOF analysis applied to the whole passage. The first mode seems to be a combination of the barotropic mode and the first baroclinic mode of the quasi-geostrophic dynamics. The second one marks the double-cell circulation structure with the NACW flowing southward and the AAIW flowing northward. Temporal amplitudes are given in Figure 6 and show a notable temporal variability, similar to that described in the original data set.

[19] Section 4.1 showed that the third significant mode in the previous EOF analysis was related to the upwelling dynamics and it is not present in the temporal EOF analysis. This fact suggests that the upwelling dynamics does not introduce relevant variability at the EBC4 mooring.

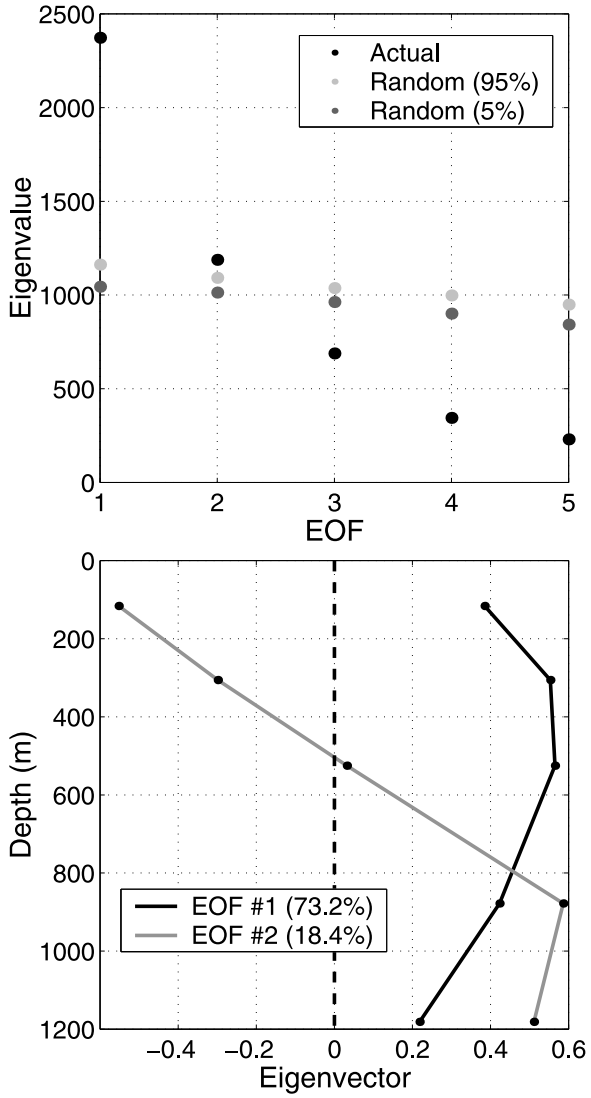

Figure 5. A temporal EOF analysis is carried out with the 9-year time series in the Lanzarote Passage. (a) The Monte Carlo Method to determine the (b) two significant oscillation modes, together with the total explained variance for each mode.

[20] Therefore, combining the spatial and temporal EOF analyses, the circulation in the passage can be described as a double-cell circulation, with the upper layer occupied by NACW and a small influence of the upwelling, and the second layer for the intermediate waters occupied by AAIW and MW. Most variability (56%) is related to the barotropic circulation and the first baroclinic mode, while the double-cell circulation and the effect of the upwelling have a weaker influence (~11–12%).

5. Periodic Signals

[21] The length of these time series is optimal for detecting long-term periodic phenomena in the passage, from seasonal to inter-annual variability. Here we try first a harmonic study, complemented later with a Wavelet analysis.

5.1. Harmonic Analysis

[22] Due to the fact that our 9-year time series has several gaps, a Fast Fourier Transform can not be used as a method to extract the harmonics in the EBC4 records. We have instead used the technique developed by *Lomb* [1976] and *Scargle* [1982] to detect the presence and significance of periodic signals in the unevenly sampled data. The justification for the use of this technique is that it provides a reasonably good approximation of the spectrum obtained by fitting sine waves using least squares to the data and plotting the reduction in the sum of the residuals against frequency. This least-squares spectrum provides the best measure of the power contributed by the different frequencies to the overall variance of the data and can be regarded as the natural extension of Fourier methods to non-uniform data. It reduces to the Fourier power spectrum in the limit of equal spacing. This method has already been applied to the very first four years of this time series [*Hernández-Guerra et al.*, 2003], and we now extend it to the nine-year record in order to detect longer period signals. The only inconvenience in this method is that it is subject to spectral leakage, i.e., the dominant peak appears at the highest frequency and also at other frequencies. Thus, a harmonic function with a period equal to the highest frequency must be subtracted from the original data. The residual is then used to compute the periodogram again and the next frequency of the data is obtained [*Lomb*, 1976; *Scargle*, 1982; *Hernández-Guerra et al.*, 2003].

[23] Table 2 shows the results of these calculations together with the amplitude, phase and total variance explained for each frequency contained in every time series. Recall that the shallowest current meter is not considered in this calculation because of the high number of gaps in the time series. The level of significance of each frequency shown in Table 2 is 99.9%. The strongest signal for the time series corresponding to the 300, 520 and 870 m depths is the annual period. Although the annual period also appears in the time series at 1230 m depth, the total variance explained for this period is less than the semi-annual signal, which seems to be dominant in the intermediate and deeper parts of the passage. A significant signal at a period of 3 months appears for each time series. The total variance explained for this period is different between the thermocline and the intermediate-deep waters. This difference is from 10% to 13% at the thermocline waters to 5.4% to 5.6%, at the intermediate and deep waters. This fact shows that the seasonal signal is very important over the whole water column, especially within the thermocline. A significant signal at a period of 2 months is present in the thermocline waters with a low contribution to the total explained variance. Finally, two more signals are present in the time series, the longest one, with an 18-month period at 300 m depth with a total explained variance of 7.3%, and the 9-month period signal that appears at 520 and 870 m depth. The contribution of this last period to the total explained variance is quite small, 1.8% and 2.3%, respectively, but significant.

5.2. Wavelet Analysis

[24] Once we have examined the periodicities in the frequency domain that have implicitly assumed that the underlying processes are stationary in time, a Wavelet

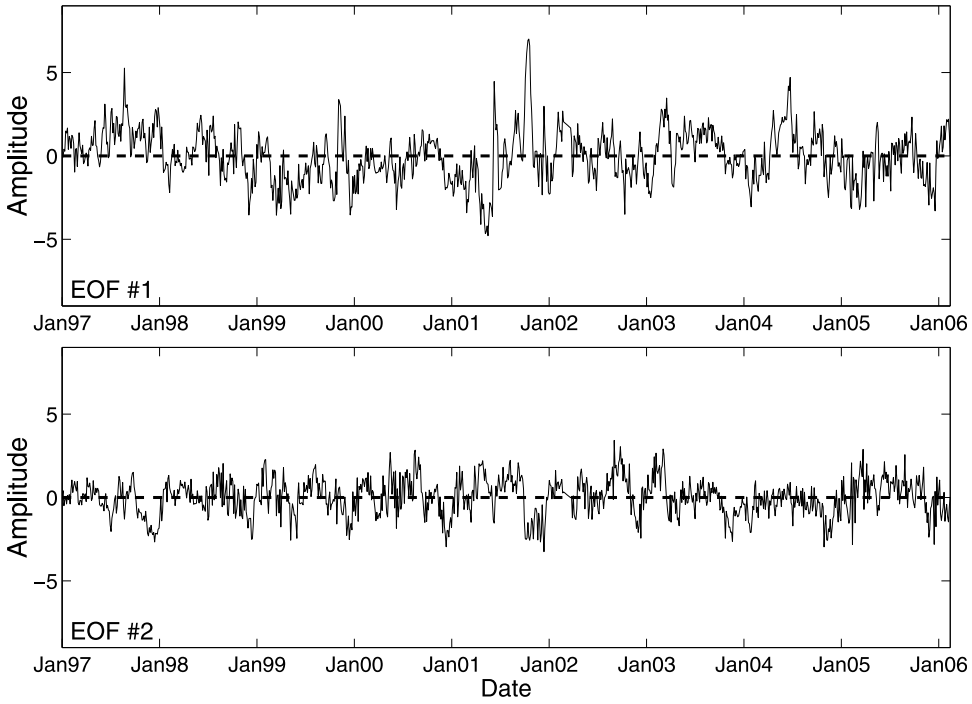

Figure 6. Amplitude corresponding to the EOF analysis for the EBC4 mooring.

analysis is applied in order to transform the expanded time series into time-frequency space, so that we can find localized intermittent periodicities [*Torrence and Compo*, 1998; *Torrence and Webster*, 1999; *Grinsted et al.*, 2004].

[25] Many statistical tests assume that the probability density function (pdf) is close to normal. Different authors point out that series far from the normal distribution produce rather unreliable and less significant results. Occasionally it can therefore be a good idea to transform the pdf of the time series. However, we caution against rashly changing the pdf. The Continuous Wavelet Transform (CWT) is applied to each EBC4 current meter, immersed in the different water masses found in the Lanzarote Passage (NACW, AAIW and MW).

[26] Figures 7a and 7b show the continuous wavelet power spectrum for the current meter immersed in the NACW. There are clearly common features in the wavelet power of the two time series such as the high power for the ~1-year (371 days) band over the whole time period, though in 2002 where the presence of this band practically

Table 2. Frequencies Contained in the 9-Year Time Series of the Component of the Velocity Along the Direction of Maximum Variance

Current Meter Depth (m)	Frequency[a]	Amplitude[b] (cm s^{-1})	Phase[b,c] (days)	Total Variance Explained (%)
300	18 (557)	1.5	183	7.3
300	12 (371)	2.1	16	11.7
300	6 (196)	1.2	−43	6.0
300	3 (79)	1.3	−60	10.0
300	2 (57)	1.4	−54	4.7
520	12 (371)	1.6	69	15.0
520	9 (278)	0.8	62	1.8
520	6 (165)	1.0	53	4.2
520	3 (79)	1.2	−73	13.0
520	2 (57)	1.1	−35	2.9
870	12 (371)	2.3	−75	19.5
870	9 (278)	0.8	−30	2.3
870	6 (185)	2.1	10	16.0
870	3 (90)	0.9	−79	5.4
1230	12 (352)	0.9	19	3.7
1230	6 (188)	1.1	69	8.0
1230	3 (94)	1.3	−81	5.6

[a]Frequency is given in months and days with the days given in parentheses.
[b]The amplitude and phase correspond to the harmonics matching the data.
[c]Phase is relative to January 1.

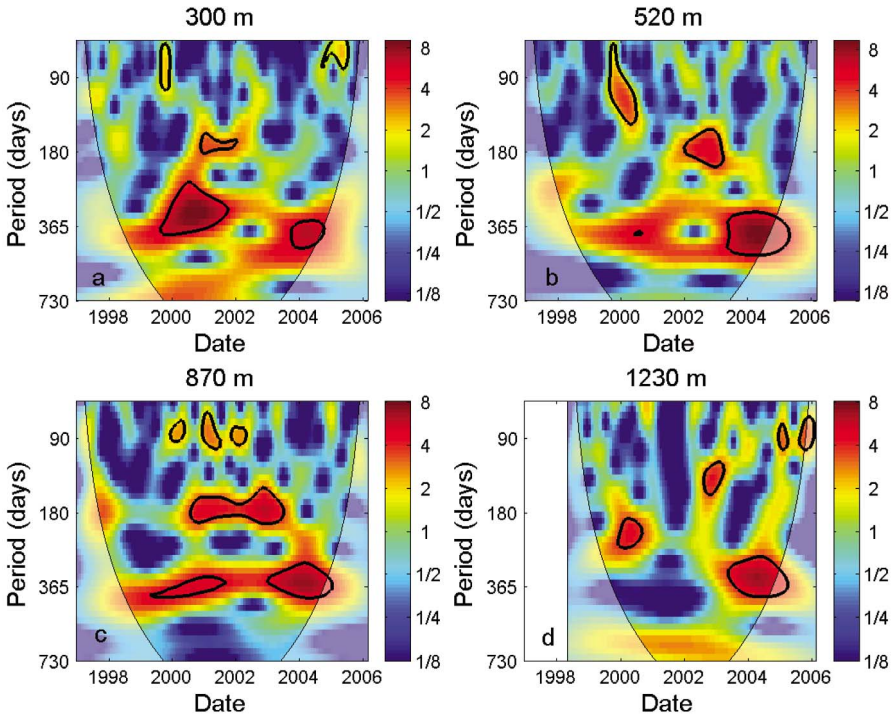

Figure 7. The continuous wavelet power spectrum for the time series of each current meter ((a–d) 2–5) at the EBC-4 mooring. The thick black contour shows the 5% significance level against red noise, and the cone of influence (COI) where edge effects might distort the picture is shown as a lighter shading.

disappears. Two significant peaks in this band are centered around 2000–2002 and 2003–2005 in both current meters. Both series also have high power in the ~9-month (278 days) band in the period from 2000–2002, though for the deeper time series the power is not above the 5% significance level. Two significant peaks in the ~6-month (165–196 days) band are localized around 2001–2002 for the shallower current meter and around 2002–2003 for the deeper time series in the NACW. Finally, similar patterns in the ~3-month (90 days) bands are found around 2000 for both current meters, and just one significant peak in 2005 for the shallower current meter.

[27] Figure 7c shows the CWT for the AAIW current meter time series with three well marked significant bands. The first one is located at the ~1-year (371 days) period from 1999–2005, except for the period of time around 2002 where the significance of the band is not above the 5% level. The second one is located in the ~6-month (185 days) period from 2000–2004 and finally, the third significant peak in the ~3-month (90 days) band is distributed along the time series with 3 significant peaks in 2000, 2001 and 2002.

[28] Figure 7d shows the CWT for the MW current meter time series. The wavelet power pattern for this current meter is quite different for the shallower current meters. The ~1-year (352 days) band is significant and appears just at the end of the time series around 2003–2005. A significant peak at the ~6-month (188 days) band is evident in 2000–2001. A significant peak that does not appear in the harmonic analysis is present in the wavelet power pattern centered at the ~135-day band and around 2003. Finally, two significant peaks at the ~3-month (94 days) band are seen in 2004 and 2005.

[29] The results obtained from this analysis agree well with the periodicities shown in Table 2 for all the current meters. However, the results add completely new information about the location in time of the periodicities first obtained.

6. Variability in Mass Transport

[30] In this section, we describe the variability in the mass transport according to both the vertical structure in the passage obtained from the EOF analysis and from the significant periodicities presented in section 5. Mass transports are estimated for the whole Lanzarote Passage by using the polynomial function obtained by *Hernández-Guerra et al.* [2003] in the three water masses present in the area. These water masses have been selected following the definition in the introduction.

6.1. Temporal Variability

[31] Figure 8 shows the temporal variability of mass transport for the NACW, AAIW and MW, respectively. Figure 8a shows the time mass transport for the thermocline water from January 1997 to February 2006. The mean mass transport is −0.81 ± 1.48 Sv, which agrees well with that obtained by *Hernández-Guerra et al.* [2003] for the first four years of the data (−0.80 ± 1.1 Sv). This fact demonstrates that the mean mass transport for the thermocline waters has not changed in the last 5 years compared with the first four. Fluctuations of the transport time series on a short time scale are large, with a maximum range from −6.65 Sv southward to +6.45 Sv northward.

[32] Figure 8b shows the 9-year variability of the mass transport for AAIW in the Lanzarote Passage with a mean

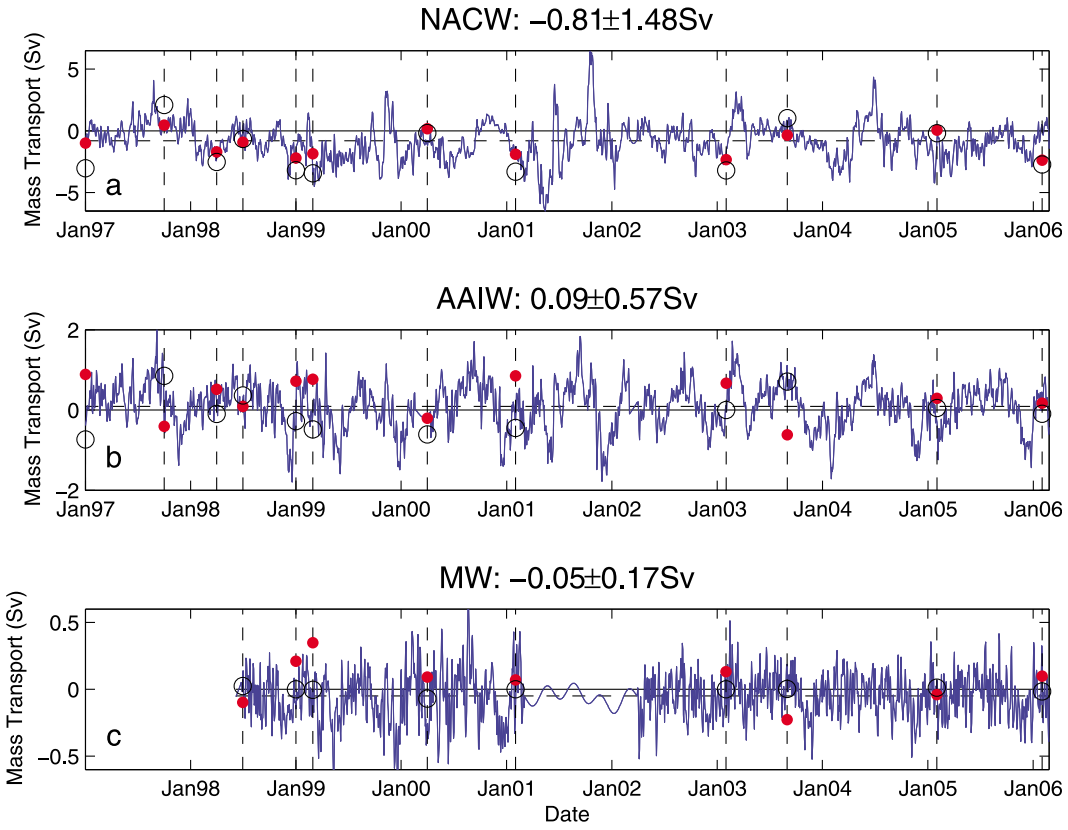

Figure 8. Estimated mass transport based at the EBC4 mooring for (a) NACW, (b) AAIW and (c) MW together with the geostrophic mass transport estimates from hydrographic stations in the Lanzarote Passage during the different surveys carried out from 1997 to 2006. The transports are smoothed with a 1-month running mean. The means and standard deviations are shown at the top. The means are also shown as a horizontal dashed line. Note that different scales are used for Figures 8a–8c. Dots represent the geostrophic mass transports computed with a level of no motion at γ_n = 27.3 kg m^{-3}, circles show the geostrophic mass transports with a level of no motion at the bottom.

value of +0.09 ± 0.57 Sv. This value also agrees with that obtained by *Hernández-Guerra et al.* [2003], indicating that the mean mass transport for AAIW in the Lanzarote Passage has not significantly changed in the last 5-year compared with the first four. The range for AAIW is from 2.0 to −2.0 Sv.

[33] Mass transport for MW is shown in Figure 8c with a mean value of −0.05 ± 0.17 Sv. This value, as for NACW and AAIW, agrees with that obtained by *Hernández-Guerra et al.* [2003]. Two significant gaps are present in the series, the first from January 1997 to June 1998 and the second from February 2001 to March 2002. The beginning of this series is considered to be at the end of the first gap (June 1998); the second gap has been interpolated using the three significant periods obtained in section 5. The range for the MW is from −0.6 to 0.6 Sv.

[34] Figure 8 also shows the geostrophic mass transports obtained from the hydrographic stations in the Lanzarote Passage as described in section 2.2. Ekman transports obtained across the Lanzarote Passage have been estimated at weekly intervals based on ERS-2 data (January 1997–June 1999) and QuikScat data (July 1999–February 2006). Ekman transport has been added to the very first layer in order to take into account the effect of the wind component on the geostrophic mass transport. Geostrophic mass transports obtained using a level of no motion at the neutral density level located between NACW and AAIW have better agreement with the 9-year mass transport of the EBC4 than those using the bottom level.

[35] *Hernández-Guerra et al.* [2002] estimated the mass transport in the thermocline layer from XBT data in the Lanzarote Passage. They estimated the mass transport every two months for two years using a θ/S relation from historical CTD data. Figure 9 shows that the XBT mass transport and the mass transport estimated from EBC4 present a similar shape, indicating that the mass transport obtained with EBC4 is in good agreement with results obtained previously with other types of data.

6.2. Seasonal Variability

[36] A canonical year is generated by averaging daily mean values over the nine years of data in order to obtain the mean monthly and seasonal variability of mass transport for NACW, AAIW and MW (Figure 10). The quantification of the seasonal mass transport for NACW, AAIW and MW during the last nine years are presented in Tables 3, 4, and 5, respectively.

[37] Figure 10a shows that the monthly mean mass transports for NACW are southward throughout the year except from late October to the beginning of November, when it is approximately null. As shown in Table 3, the

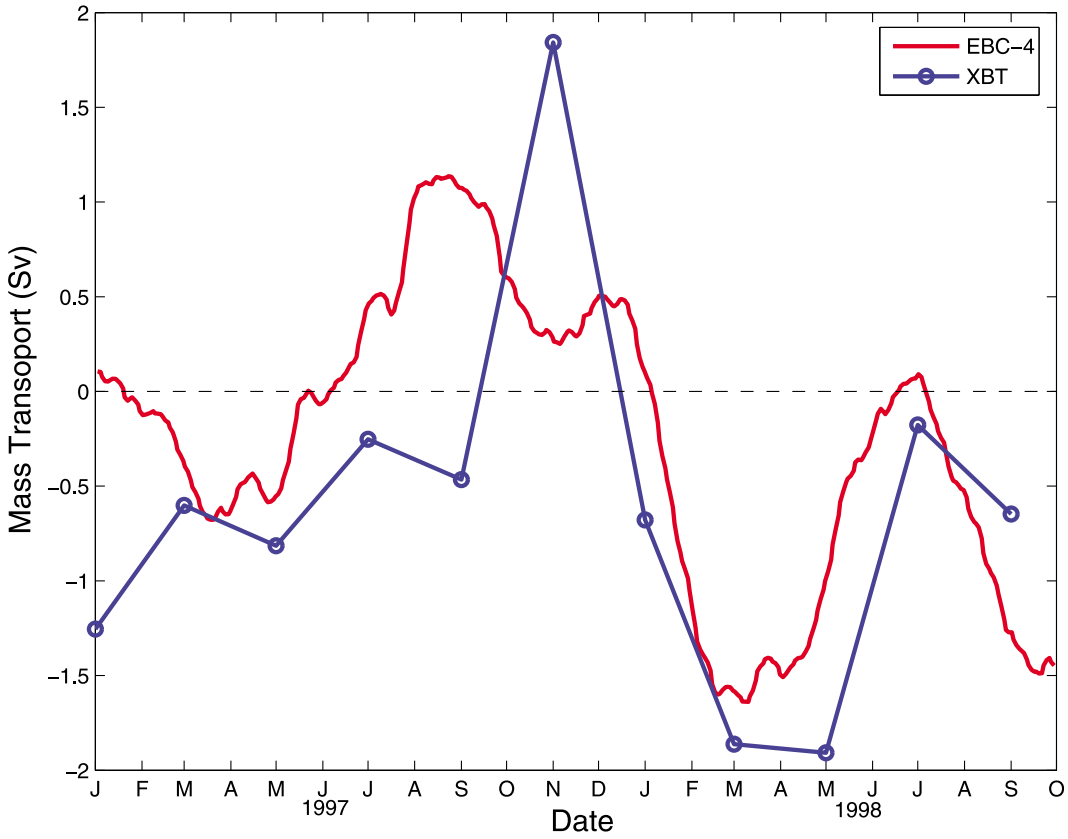

Figure 9. Estimated mass transport based on the EBC-4 mooring for NACW, and the estimates obtained from XBT data and a θ/S relation from historical CTD data. A running filter of 1-month has been applied to the mass transport from the EBC4 data.

seasonal mass transport is maximum in winter (−1.30 ± 1.29 Sv), decreasing in spring (−0.99 ± 1.59 Sv) and summer (−0.57 ± 1.13 Sv), and having its minimum value in fall (−0.44 ± 1.50 Sv).

[38] Monthly mass transports for AAIW are shown in Figure 10b that present a different pattern than NACW. Northward transport is observed along the year except from November to January. December is the month with maximum southward transport of −0.65 Sv. Maximum northward transports of +0.53 Sv and +0.50 Sv are found in August and September, respectively. At the seasonal scale, Table 4 shows that winter has a practically null mass transport of +0.02 ± 0.47 Sv. During spring and summer, mass transport of AAIW is northward with a mean value of +0.12 ± 0.48 Sv and +0.44 ± 0.37 Sv, respectively. In contrast, winter has a southward transport of −0.23 ± 0.57 Sv.

[39] Figure 10c shows the monthly mean transport for MW. Transport is very low with a maximum southward transport in December (−0.19 ± 0.15 Sv). Mean seasonal transport is always southward (Table 5) ranging from −0.01 ± 0.10 Sv in summer to −0.04 ± 0.11 Sv in spring. Nonetheless, southward mass transport in fall is three times greater than that found in spring (−0.12 ± 0.12 Sv).

6.3. Inter-Annual Variability

[40] Figure 11 shows the inter-annual variability of mass transports computed as cumulative monthly mass transports for each water mass. 9-year time series have been divided into 5 different periods of time: P1, from January 1997 to September 1998, P2, from September 1998 to July 2000, P3, from July 2000 to March 2003, P4, from March 2003 to November 2003 and P5, from November 2003 to February 2006. These different periods correspond to changes in the cumulative mass transport trends respect to the 9-years mean mass transports for the different water masses.

[41] Figure 11a shows a practically null accumulated mass transport for NACW for the period P1. During P2, there is a clear monotonic increase of accumulated mass transport. The yearly mean in this period, −1.50 Sv, is double the 9-year mean. During P3, the slope of the NACW accumulated mass transport decreases and the yearly mean, −0.83 Sv, is close to the 9-year mean. P4 has a null accumulated mass transport, similar to P1. During P5, the yearly mean mass transport is similar to the 9-year mean mass transport.

[42] Figure 11b shows a tripling of the AAIW mass transport trend during P1, with a mean value around +0.28 Sv. During P2, a change of sign in the AAIW trend is found with a mean value of −0.09 Sv. This change in the sign of the trend is followed by a new change in the trend during P3, when the 9-year mean trend for AAIW is recovered. P4 is characterized by a quadrupling of the mean trend, with a value around +0.39 Sv. Finally, during P5, the cumulative mass transport of AAIW keeps increasing its value following the 9-year mean trend. The cumulative mass transport of AAIW clearly shows the maximum values obtained for this water mass during November over the whole time series, as well as the minimum values in January.

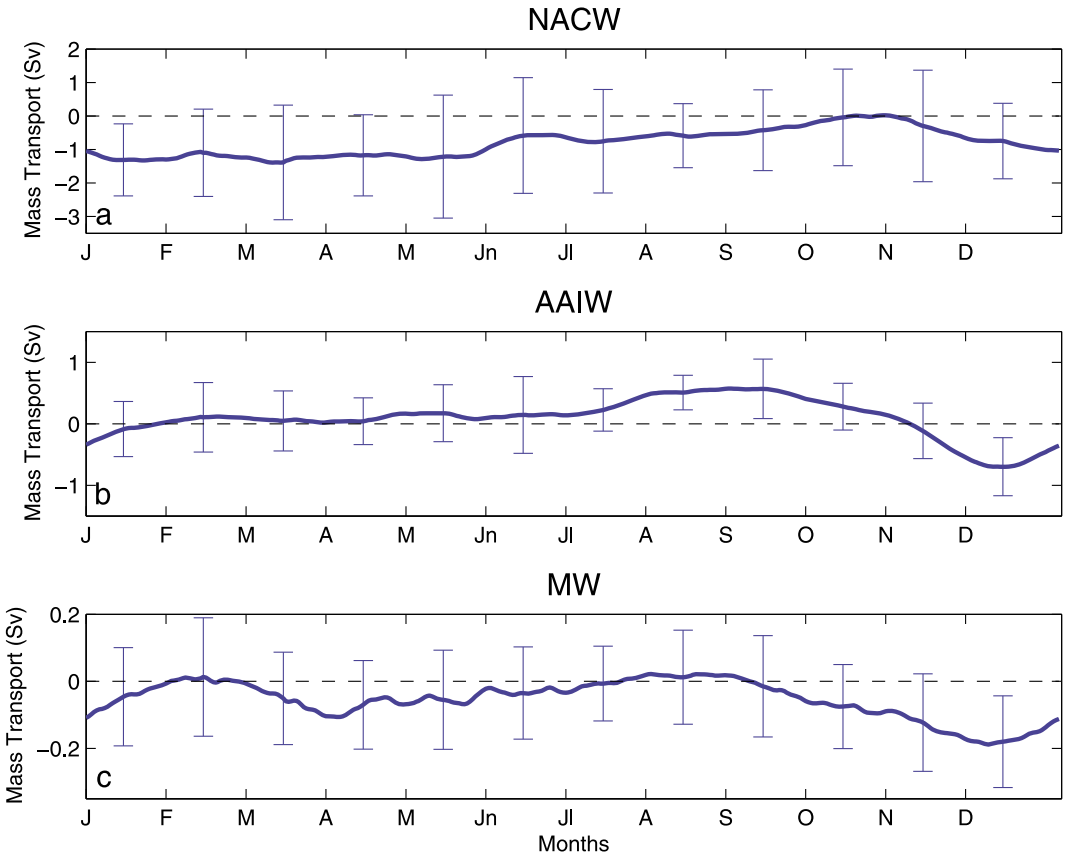

Figure 10. Seasonal variability of the mass transport computed with daily means for each year for (a) NACW, (b) AAIW, and (c) MW. Monthly variability is shown as a standard deviation for every month. Note that different scales are used for Figures 10a–10c.

[43] Figure 11c shows the cumulative mass transport of MW, which follows the same pattern as the cumulative mass transport of NACW. A gap in the initial velocities is found in P1, so the mass transport could not be obtained. During P2, the mean trend almost doubles the 9-year mean of MW mass transport, −0.08 Sv. P3 and P5 follow the 9-year mean of the mass transport, with a mean value of −0.05 Sv. During P4 a practically null mean mass transport in the MW is found.

7. Results and Discussion

[44] In this study, one of the longest current meter velocities time series in the Eastern North Atlantic Subtropical Gyre have been used to quantify the 9-year, interannual and seasonal mass transport variability for NACW, AAIW and MW measured in the Lanzarote Passage. *Hernández-Guerra et al.* [2003] published the annual mean mass transport in the passage for the first four years of the full data record. These values were −0.8 ± 1.1 Sv to the south for NACW, +0.1 ± 0.4 Sv to the north for AAIW, and −0.05 ± 0.09 Sv to the south for MW. At present, the EBC4 mooring record has 5 more years of information, and reveals that the yearly mean mass transport for the three water masses present in the area has not changed significantly over the last5 years. The new annual mean mass transports quantified in this study are: −0.81 ± 1.48 Sv for NACW, +0.09 ± 0.57 Sv for AAIW and −0.05 ± 0.17 Sv for MW. Two different data sets have corroborated the mass transports

Table 3. Seasonal, Annual, and 9-Year Mean Mass Transports for NACW From 1997 to 2005[a]

Years	Winter	Spring	Summer	Fall	Annual
1997	−0.24 ± 0.45	−0.28 ± 0.78	+0.92 ± 0.78	+0.48 ± 0.59	+0.22 ± 0.83
1998	−1.25 ± 0.90	−0.62 ± 0.81	−0.84 ± 0.77	−0.98 ± 1.07	−0.92 ± 0.92
1999	−1.69 ± 1.42	−2.21 ± 0.42	−1.32 ± 0.96	−0.91 ± 2.15	−1.53 ± 1.47
2000	−1.42 ± 0.81	−1.77 ± 0.80	−1.41 ± 0.87	+0.51 ± 0.42	−1.02 ± 1.16
2001	−1.78 ± 0.94	−2.66 ± 2.73	−0.96 ± 1.31	+0.86 ± 2.52	−1.14 ± 2.41
2002	−0.89 ± 1.05	−0.43 ± 0.80	−0.42 ± 0.74	−1.26 ± 0.85	−0.75 ± 0.93
2003	−0.00 ± 1.69	−0.07 ± 0.78	−0.03 ± 0.48	−0.89 ± 0.39	−0.25 ± 1.04
2004	−2.31 ± 0.76	+0.36 ± 0.71	−0.42 ± 1.35	−0.55 ± 0.91	−0.73 ± 1.56
2005	−2.13 ± 0.92	−1.21 ± 0.71	−0.61 ± 0.61	−1.25 ± 0.82	−1.30 ± 0.94
9-year mean	−1.30 ± 1.29	−0.99 ± 1.59	−0.57 ± 1.13	−0.44 ± 1.50	−0.81 ± 1.48

[a]NACW, surface-27.3 kg m^{-3}; 0–600 m.

Table 4. Seasonal, Annual, and 9-Year Mean Mass Transports for AAIW From 1997 to 2005[a]

Years	Winter	Spring	Summer	Fall	Annual
1997	+0.24 ± 0.23	+0.34 ± 0.35	+0.68 ± 0.38	−0.23 ± 0.36	+0.26 ± 0.47
1998	+0.20 ± 0.17	+0.36 ± 0.23	+0.29 ± 0.36	−0.28 ± 0.63	+0.14 ± 0.46
1999	+0.22 ± 0.36	−0.48 ± 0.50	+0.27 ± 0.25	−0.26 ± 0.56	−0.06 ± 0.54
2000	−0.21 ± 0.28	+0.06 ± 0.38	+0.64 ± 0.33	+0.00 ± 0.68	+0.13 ± 0.54
2001	−0.26 ± 0.33	−0.08 ± 0.59	+0.59 ± 0.48	−0.36 ± 0.77	−0.03 ± 0.68
2002	+0.14 ± 0.47	−0.03 ± 0.32	+0.34 ± 0.34	−0.06 ± 0.48	+0.10 ± 0.43
2003	+0.45 ± 0.61	+0.12 ± 0.38	+0.57 ± 0.27	−0.32 ± 0.37	+0.20 ± 0.55
2004	−0.43 ± 0.47	+0.45 ± 0.42	+0.19 ± 0.28	−0.26 ± 0.52	−0.02 ± 0.55
2005	−0.20 ± 0.35	+0.31 ± 0.23	+0.44 ± 0.27	−0.33 ± 0.53	+0.05 ± 0.49
9-year mean	+0.02 ± 0.47	+0.12 ± 0.48	+0.44 ± 0.37	−0.23 ± 0.57	+0.09 ± 0.57

[a]AAIW, 27.3–27.7 kg m^{-3}; 600–1100 m.

obtained at the EBC4 mooring in the Lanzarote Passage. First, geostrophic mass transports obtained from 12 hydrographic sections in the passage during 1997–2006 and, secondly, the computed mass transports for NACW obtained from XBT data and the θ/S relation from historical CTD data, which demonstrated for the first time the NACW flow reversal in November in the Lanzarote Passage.

[45] A canonical year has been generated by averaging daily mean values over the nine years of data in order to obtain the mean monthly and seasonal variability of the mass transport for the three water masses present in the Lanzarote Passage. The NACW seasonal pattern is characterized by a maximum southward transport in winter (−1.30 ± 1.29 Sv), decreasing in spring and summer, with the minimum mass transport in fall (−0.44 ± 1.50 Sv). This pattern differs from that expected given the Trade winds seasonal variability, which presents its maximum intensity during summer. The offshore diversion of the southward Canary Current at Cape Ghir might be a plausible explanation for this seasonal pattern found in the Lanzarote Passage [*Navarro-Pérez and Barton*, 2001]. On this basis, *Pelegrí et al.* [2005] have also suggested that by late fall, southward transport of the Canary Current is maximum and the flow becomes unstable and separates from the coast, retaking its southward motion further west between the central or western Canary Islands. At this time, the Lanzarote Passage might support northward transports as shown in Table 3. Similar results has been obtained by a high resolution numerical model in the area of study [*Mason*, 2009].

[46] Seasonal mass transport for AAIW shows notable differences with respect to the NACW pattern. During winter, when the NACW mass transport reaches its maximum southward value, AAIW mean mass transport is practically zero (+0.02 ± 0.47 Sv) although the root mean square is 0.28 Sv. This fact reflects that during winter, the mass transport of AAIW has a mean intensity of 0.28 Sv with a north/south direction (northward +0.25 Sv/southward −0.28 Sv). During spring and summer, the mass transport of AAIW is northward with a 9-year mean values of around +0.12 ± 0.48 Sv and +0.44 ± 0.37 Sv, respectively. August and September are the summertime months where a maximum northward AAIW flow is found over the whole time series. After this northward intensification of AAIW mass transport, a southward transport is found in December over the whole time series, with a mean value of −0.66 ± 0.49 Sv. MW over the first half of a year has seasonal mean mass transports of −0.03 ± 0.11 Sv and −0.04 ± 0.11 Sv, for winter and spring, respectively. During summer, a reduction of a flow is found with a mean value of −0.01 ± 0.10 Sv rapidly increasing in fall to a mean value of −0.12 ± 0.12 Sv. The maximum value is reached in December, −0.19 ± 0.15 Sv. The two deepest current meters and salinity records of the EBC4 mooring for the same period of time of our study have been used by *Machín and Pelegrí* [2009] and *Machín et al.* [2010] to explain the seasonal variability of the intermediate waters. These authors have confirmed by means of a Sverdrup-type model that the summer northward progression of AAIW by a fall intense flow reversal of MW is associated to stretching or shrinking of the intermediate water strata.

[47] The inter-annual variability of the mass transport suggests the existence of 5 different periods of time where the cumulative monthly mass transport trend changes for the three water masses present in the area (P1–P5, Figure 11). During the P1 and P4 time periods the mass transport for NACW and MW is practically null; however, during the same period of time, the AAIW 9-year mean trend mass

Table 5. Seasonal, Annual, and 9-Year Mean Mass Transports for MW From 1997 to 2005[a]

Years	Winter	Spring	Summer	Fall	Annual
1997	-	-	-	-	-
1998	-	+0.01 ± 0.01	−0.03 ± 0.08	−0.12 ± 0.10	−0.04 ± 0.08
1999	−0.05 ± 0.15	−0.13 ± 0.15	−0.01 ± 0.09	−0.21 ± 0.17	−0.10 ± 0.16
2000	+0.01 ± 0.15	−0.09 ± 0.19	+0.05 ± 0.20	−0.14 ± 0.16	−0.04 ± 0.19
2001	−0.04 ± 0.15	−0.04 ± 0.04	−0.02 ± 0.04	−0.09 ± 0.03	−0.04 ± 0.09
2002	−0.07 ± 0.06	−0.09 ± 0.12	−0.02 ± 0.11	−0.10 ± 0.08	−0.07 ± 0.10
2003	+0.01 ± 0.10	−0.03 ± 0.10	+0.03 ± 0.07	−0.13 ± 0.11	−0.03 ± 0.11
2004	−0.01 ± 0.10	−0.01 ± 0.08	−0.05 ± 0.11	−0.13 ± 0.12	−0.05 ± 0.11
2005	−0.07 ± 0.10	+0.01 ± 0.08	−0.01 ± 0.08	−0.14 ± 0.11	−0.05 ± 0.11
9-year mean	−0.03 ± 0.11	−0.04 ± 0.11	−0.01 ± 0.10	−0.12 ± 0.12	−0.05 ± 0.17

[a]MW, $\gamma_n > 27.45$ kg m^{-3}; 900-bottom.

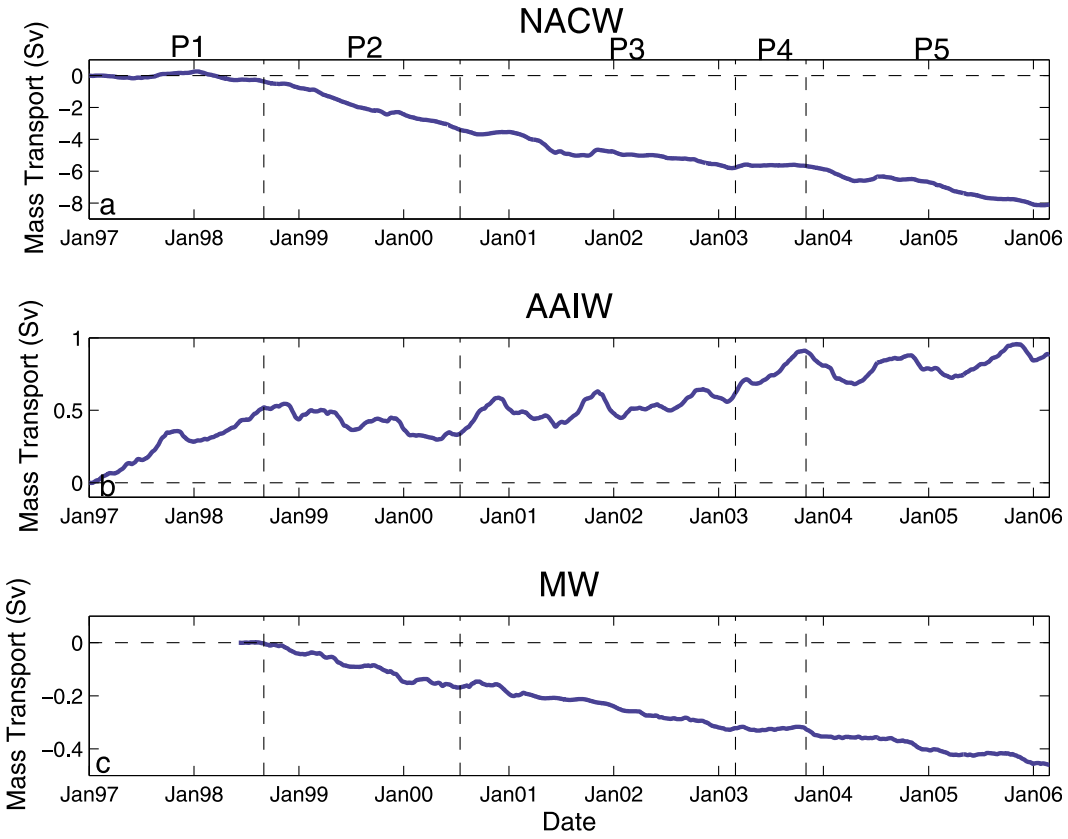

Figure 11. Inter-annual variability of the mass transports computed as cumulative monthly means for each year for (a) NACW, (b) AAIW and (c) MW.

transport increases by factors of 3 and 4, respectively. During P2, the accumulated mass transport trend for NACW and MW starts increasing by a factor of 2, while the AAIW trend changes its sign. Finally, during P3 and P5, NACW, AAIW and MW return to the normal 9-year mean trend.

[48] The P-Periods described in this study seem to be related to the instability of the Canary Current north of the Canary Archipelago, as we have commented on above, together with the combination of the different phases of the North Atlantic Oscillation (NAO) index. Positive NAO phases are found during all of the periods except P2. During these positive phases, the predominant northeastern Trade Winds are intensified [*Czaja and Marshall*, 2000], reducing the southward NACW mass transport at the Lanzarote Passage and favoring the northward mass transport of the AAIW. During late 1998 to mid 2000 (P2), a negative NAO phase is found which might be related to the increasing of the NACW mean mass transport trend. However, further investigation is needed in order to demonstrate the significance of this relationship.

[49] Results from the first year of the RAPID/MOCHA array have demonstrated the ability of the observing system to continuously measure the strength and vertical structure of the Atlantic MOC [*Kanzow et al.*, 2007; *Chidichimo et al.*, 2010]. The inter-annual variability in the Atlantic MOC should be defined with a resolution of 1.5 Sv [*Cunningham et al.*, 2007] because that is the order of magnitude of mass transport fluctuation in the Lanzarote Passage. On this basis, and in order to conclude this study, the strong transport fluctuations at seasonal and inter-annual time scales in the Eastern Boundary Current of the North Atlantic Subtropical Gyre demonstrates that the Eastern Boundary Current transport has a significant impact on meridional overturning estimates, indicating that in order to understand MOC variability, transport estimates in the eastern Atlantic margin are necessary.

[50] **Acknowledgments.** This study has been performed as part of the Instituto Español de Oceanografía RAPROCAN Project, European Union through CANIGO (MAS-CT96-0060) project and the Spanish Ministry of Science though Argo-Spain (ICTS-2008-14) and ORCA (CTM2005-04701-C02-01) projects. The authors would like to thank the invaluable comments of José Luis Pelegrí as well as the officers and crew of the R/V *Cornide de Saavedra* for their help at sea.

References

Arhan, M., A. Colin de Vèrdiere, and L. Mémery (1994), The eastern boundary of the subtropical North Atlantic, *J. Phys. Oceanogr.*, *24*, 1295–1316.

Chidichimo, M. P., T. Kanzow, S. A. Cunningham, and J. Marotzke (2010), The contribution of eastern-boundary density variations to the Atlantic meridional overturning circulation at 26.5°N, *Ocean Sci.*, *6*, 475–490.

Cunningham, S. A., et al. (2007), Temporal variability of the Atlantic meridional overturning circulation at 26.5°N, *Science*, *317*(5840), 935–938.

Czaja, A., and J. Marshall (2000), On the interpretation of AGCMs response to prescribed time-varying SST anomalies, *Geophys. Res. Lett.*, *27*, 1927–1930.

Emery, W., and R. E. Thomson (1998), *Data Analysis Methods in Physical Oceanography*, 634 pp., Elsevier, New York.

Fraile-Nuez, E., and A. Hernández-Guerra (2006), Wind-driven circulation for the eastern North Atlantic Subtropical Gyre from Argo data, *Geophys. Res. Lett.*, *33*, L03601, doi:10.1029/2005GL025122.

Grinsted, A., J. C. Moore, and S. Jevrejeva (2004), Application of the cross wavelet transform and wavelet coherence to geophysical time series, *Nonlinear Processes Geophys.*, *11*, 561–566.

Hammersley, J., and D. Handscomb (1964), *Monte Carlo Methods*, 178 pp., Wiley, London.

Hernández-Guerra, A., and L. Nykjaer (1997), Sea surface temperature variability off north-west Africa: 1981–1989, *Int. J. Remote Sens.*, *18*(12), 2539–2558.

Hernández-Guerra, A., F. López-Laatzen, F. Machín, D. de Armas, and J. L. Pelegrí (2001), Water masses, circulation and transport in the Eastern Boundary Current of the North Atlantic Subtropical Gyre, *Sci. Mar.*, *65*, suppl. 1, 177–186.

Hernández-Guerra, A., et al. (2002), Temporal variability of mass transport in the Canary Current, *Deep Sea Res. Part I*, *49*, 3415–3426.

Hernández-Guerra, A., E. Fraile-Nuez, R. Borges, F. López-Laatzen, P. Vélez-Belchí, G. Parrilla, and T. J. Müller (2003), Transport variability in the Lanzarote passage (Eastern Boundary Current of the North Atlantic Subtropical Gyre), *Deep Sea Res. Part I*, *50*, 189–200.

Hernández-Guerra, A., E. Fraile-Nuez, F. López-Laatzen, A. Martínez, G. Parrilla, and P. Vélez-Belchí (2005), Canary Current and North Equatorial Current from an inverse box model, *J. Geophys. Res.*, *110*, C12019, doi:10.1029/2005JC003032.

Jackett, D., and T. J. McDougall (1997), A neutral density variable for the world's ocean, *J. Phys. Oceanogr.*, *27*, 237–263.

Kanzow, T., S. A. Cunningham, D. Rayner, J. J. M. Hirschi, W. E. Johns, M. O. Baringer, H. L. Bryden, L. M. Beal, C. S. Meinen, and J. Marotzke (2007), Observed flow compensation associated with the MOC at 26.5°N in the Atlantic, *Science*, *317*(5840), 938–941.

Kawase, M., and J. Sarmiento (1985), Nutrients in the Atlantic thermocline, *J. Geophys. Res.*, *90*, 8961–8979.

Knoll, M., A. Hernández-Guerra, B. Lenz, F. López-Laatzen, F. Machín, T. Müller, and G. Siedler (2002), The Eastern Boundary Current system between the Canary Islands and the African Coast, *Deep Sea Res. Part II*, *49*, 3427–3440.

Laiz, I., P. Sangrà, J. L. Pelegrí, and A. Marrero-Díaz (2001), Sensitivity of an idealised subtropical gyre to the eastern boundary conditions, *Sci. Mar.*, *65*, 187–194.

Lomb, N. R. (1976), Least-squares frequency analysis of unequally spaced data, *Astrophys. Space Sci.*, *39*, 447–462.

Lozier, M. S., W. B. Owens, and R. Curry (1995), The climatology of the North Atlantic, *Prog. Oceanog.*, *36*, 1–44.

Machín, F., and J. L. Pelegrí (2009), Northward penetration of Antarctic Intermediate Water off northwest Africa, *J. Phys. Oceanogr.*, *39*, 512–535.

Machín, F., A. Hernández-Guerra, and J. L. Pelegrí (2006), Mass fluxes in the Canary Basin, *Prog. Oceanogr.*, *70*, 416–447.

Machín, F., E. Fraile-Nuez, J. L. Pelegrí, P. Velez-Belchí, F. López-Laatzen, and A. Hernández-Guerra (2010), Fall flow reversals at intermediate waters in the Lanzarote Passage from a nine-year record, *J. Phys. Oceanogr.*, doi:10.1175/2010JPO4320.1, in press.

Mason, E. (2009), High-resolution modelling of the Canary Basin oceanic circulation, Ph.D. thesis, Universidad de Las Palmas de Gran Canaria, Las Palmas, Spain.

Müller, T. J., and G. Siedler (1992), Multi-year current time series in the eastern North Atlantic Ocean, *J. Mar. Res.*, *50*, 63–98.

Navarro-Pérez, E., and E. D. Barton (2001), Seasonal and interannual variability of the Canary Current, *Sci. Mar.*, *65*, 205–213.

Paillet, J., and H. Mercier (1997), An inverse model of the eastern North Atlantic general circulation and thermocline ventilation, *Deep Sea Res. Part I*, *44*, 1293–1328.

Parrilla, G., S. Neuer, P. Y. Le Traon, and E. Fernández-Suarez (2002), Topical studies in oceanography: Canary Islands Azores Gibraltar Observations (CANIGO). Volume 1: studies in the northern Canary Islands basin, *Deep Sea Res. Part II*, *49*, 3409–3413.

Pelegrí, J. L., J. Arístegui, L. Cana, M. González-Dávila, A. Hernández-Guerra, S. Hernández-León, A. Marrero-Díaz, M. F. Montero, P. Sangrà, and M. Santana-Casiano (2005), Coupling between the open ocean and the coastal upwelling region off northwest Africa: Water recirculation and offshore pumping of organic matter, *J. Mar. Syst.*, *54*, 3–37.

Reid, J. L. (1994), On the total geostrophic circulation of the North Atlantic Ocean: Flow patterns, tracers, and transports, *Prog. Oceanogr.*, *33*, 1–92.

Scargle, J. D. (1982), Studies in astronomical time series analysis in statistical aspects of spectral analysis of unevenly spaced data, *Astrophys. J.*, *263*, 835–853.

Siedler, G., and R. Onken (1996), Eastern recirculation, in The Warm Water Sphere of the North Atlantic Ocean, edited by W. Krauss, pp. 339–364, Gebrüder Borntraeger, Berlin.

Smith, W., and D. Sandwell (1997), Global sea floor topography from satellite altimetry and ship depth soundings, *Science*, *277*(5334), 1956–1962.

Tomczak, M. (1981), An analysis of mixing in the frontal zone of South and North Atlantic central water off Northwest Africa, *Prog. Oceanogr.*, *10*, 173–192.

Torrence, C., and G. P. Compo (1998), A practical guide to wavelet analysis, *Bull. Am. Meteorol. Soc.*, *79*, 61–78.

Torrence, C., and P. J. Webster (1999), Interdecadal changes in the ENSO-monsoon system, *J. Clim.*, *12*, 2679–2690.

van Aken, H. M. (2000), The hydrography of the mid-latitude Northeast Atlantic Ocean: Part II: The intermediate water masses, *Deep Sea Res. Part I*, *47*, 789–824.

Wright, R. W., and L. V. Worthington (1970), The water masses of the North Atlantic Ocean: A volumetric census of temperature and salinity, *Ser. Atlas Mar. Environ. 19*, Am. Geophys. Soc., New York.

E. Fraile-Nuez, F. López-Laatzen, and P. Vélez-Belchí, Centro Oceanográfico de Canarias, Instituto Español de Oceanografía, General Gutiérrez 4, E-38005 Santa Cruz Spain. (eugenio.fraile@oceanografia.es; federico.lopez@ca.ieo.es; pedro.velez@ca.ieo.es)

F. Machín, Institut de Ciènces del Mar, Passeig maritim de la Barceloneta 37-49, E-08003 Barcelona, Spain. (fmachin@icm.csic.es)

V. Benítez-Barrios, R. Borges, and A. Hernández-Guerra, Facultad de Ciencias del Mar, Universidad de Las Palmas de Gran Canaria, E-35017 Las Palmas, Spain. (veronica.benitez102@doctorandos.ulpgc.es; rbormen@gmail.com; ahernandez@dfis.ulpgc.es)